Supplementary Figures for:

A broadband cavity-enhanced spectrometer for atmospheric trace gas measurements and Rayleigh scattering cross sections in the cyan region (470-540 nm)

Nick Jordan[1], Connie Z. Ye,[1] Satyaki Ghosh,[1] Rebecca Washenfelder,[2] Steven S. Brown,[2] and Hans D. Osthoff[1]

[1]Department of Chemistry, University of Calgary, 2500 University Drive NW, Calgary, AB T2N 1N4, Canada

[2]Earth System Research Laboratory, National Oceanic and Atmospheric Administration, Boulder, CO 80303, USA

Correspondence: Hans D. Osthoff (hosthoff@ucalgary.ca)

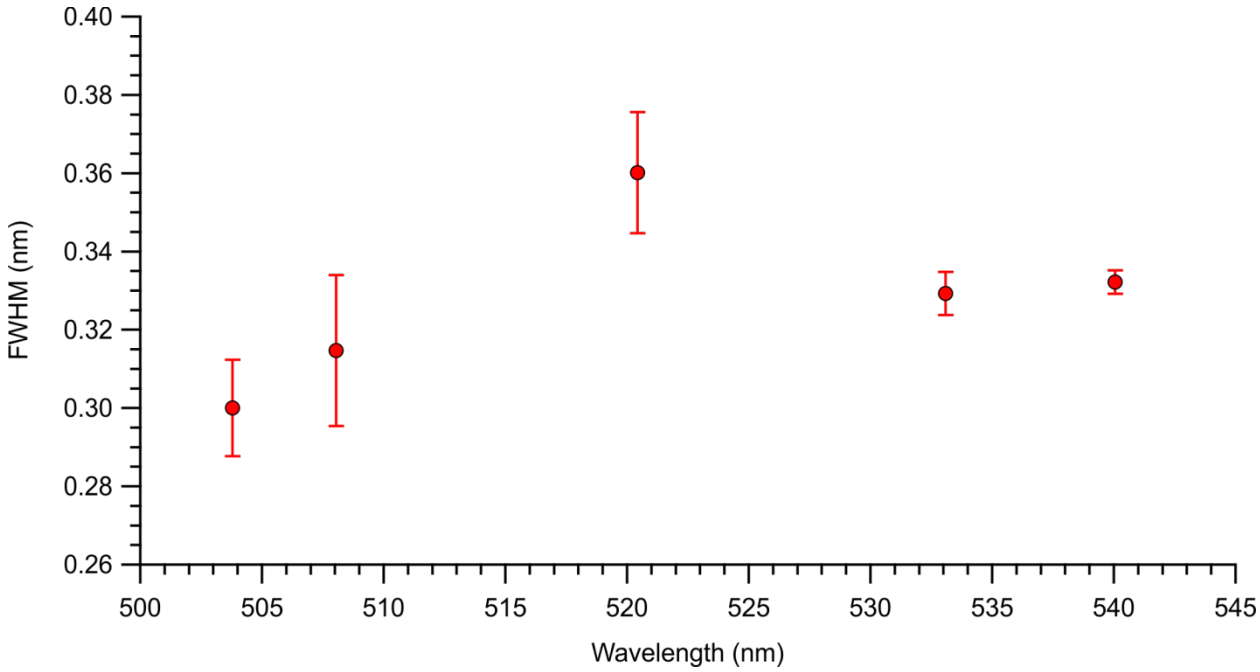

Figure S1 Full width half maximum (FWHM = 2 × width × $(\ln(2))^{1/2}$) values calculated for sharp peaks in the Hg(Ne) calibration source and 50 µm spectrometer slit width. The error bars represent 1σ of the Gaussian peak fitted to each line in the lamp spectrum.

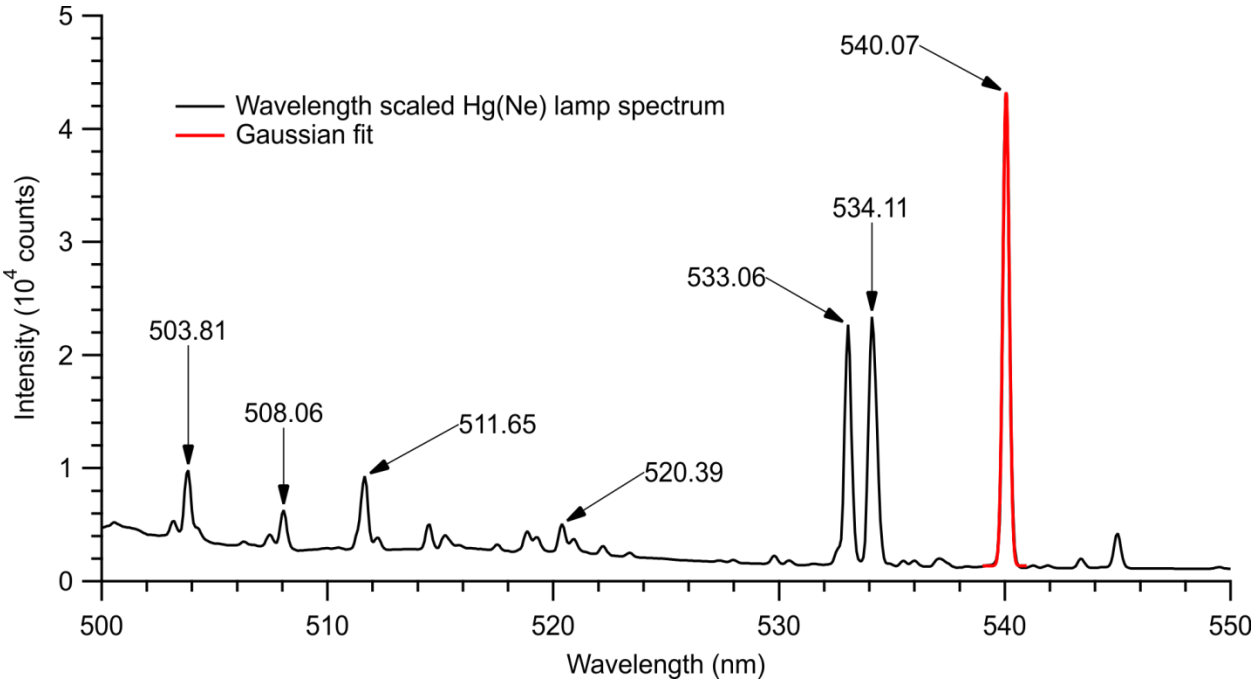

Figure S2 Wavelength calibrated Hg(Ne) lamp spectrum recorded using Acton SP2156 spectrograph equipped with PIXIS 100B CCD camera. The spectrum was produced by the average of 120 one second scans.

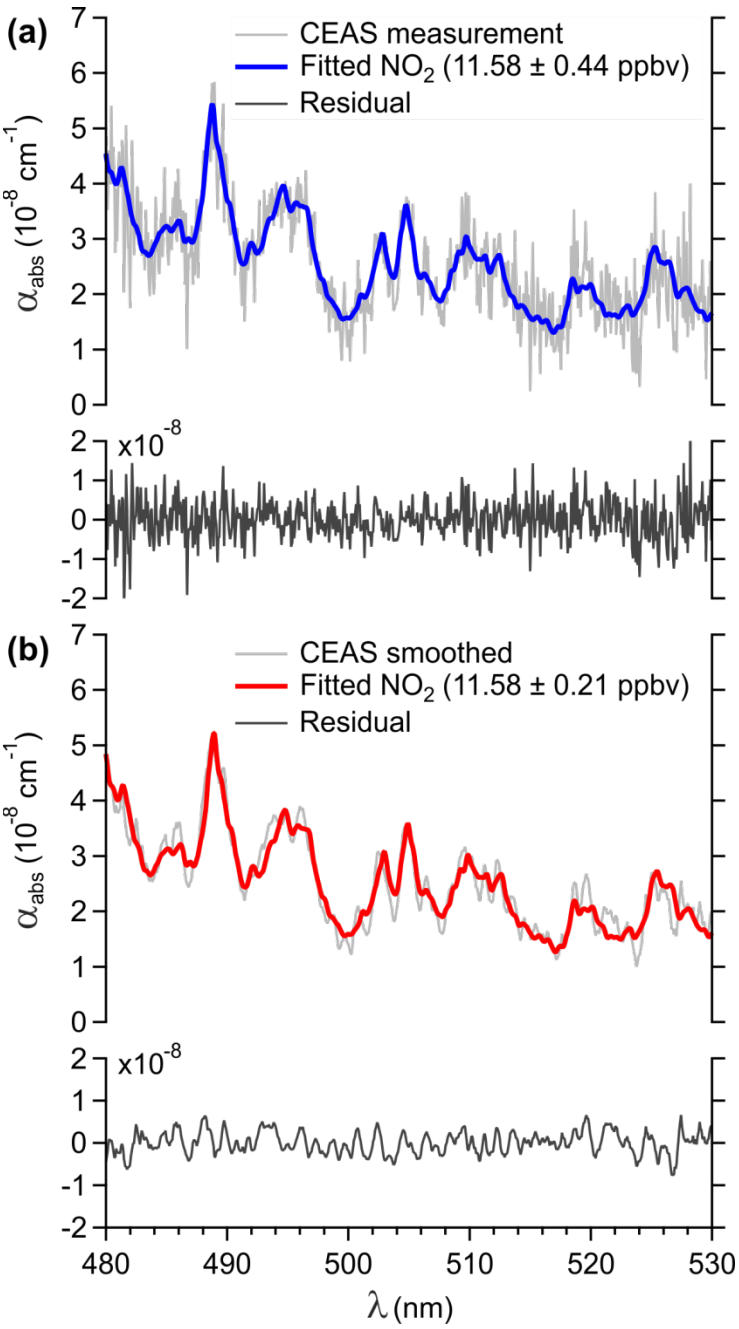

Figure S3 Example of fitted spectra for **a)** NO_2 without smoothing and **b)** NO_2 with smoothing using a fourth degree polynomial Savitzky-Golay (1964) filter.

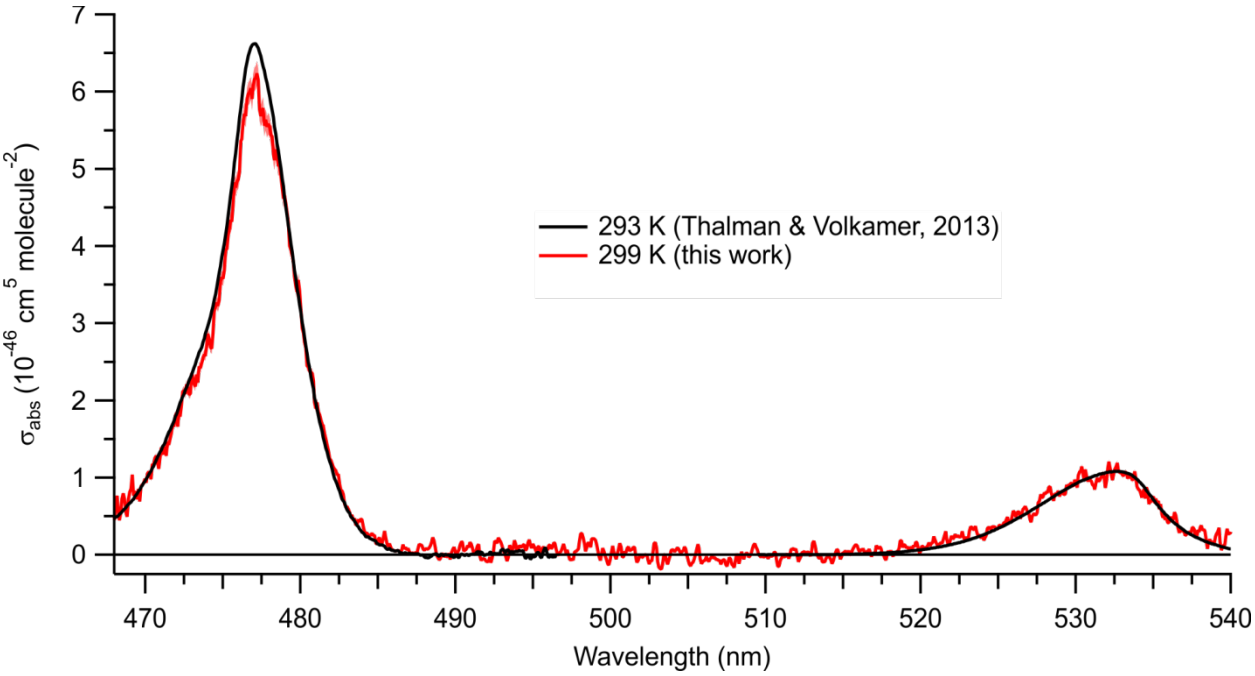

Figure S4 Room-temperature absorption cross-section of O_4, calculated from the data shown in Figure 4c. Data from (Thalman and Volkamer, 2013) are superimposed.

Table S1. Selected absorption cross-sections of O_4 at room temperature in the recent literature.

Reference	**Peak σ(477 nm)** (10^{-46} cm^5 molecule^{-2})	**Peak σ(532 nm)** (10^{-46} cm^5 molecule^{-2})
Greenblatt, 1990 (Greenblatt et al., 1990)	6.3±0.6	1.0±0.1
Newnham and Ballard, 1998 @283K (Newnham and Ballard, 1998)	8.3±0.8	1.2±0.4
Hermans et al., 1999 (Hermans et al., 1999)	6.6	1.1
Sneep and Ubachs, 2005 (Sneep and Ubachs, 2005)	-	1.01±0.03
Sneep et al., 2006 (Sneep et al., 2006)	6.60±0.06	-
Thalman and Volkamer, 2013 (Thalman and Volkamer, 2013)	6.6±0.1	1.09±0.06
This work	6.2±0.5	1.08±0.09

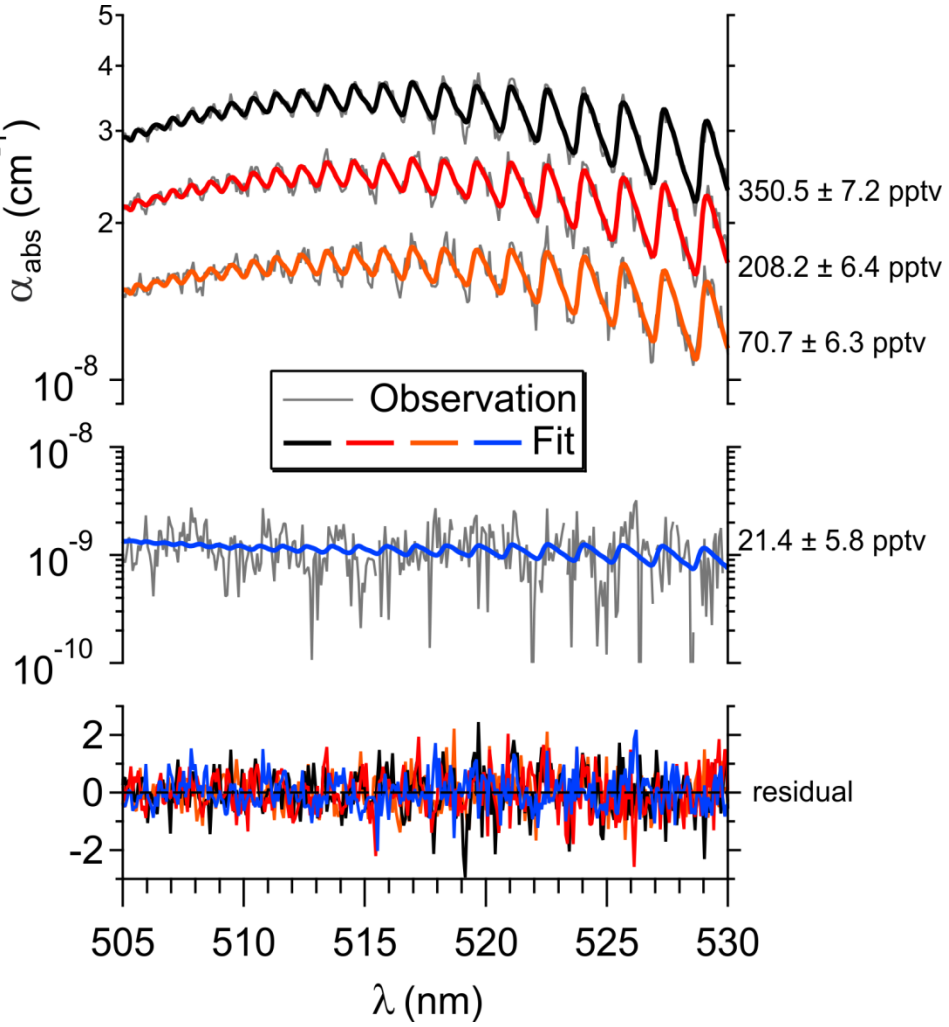

Figure S5 Spectral fits of laboratory generated I_2.

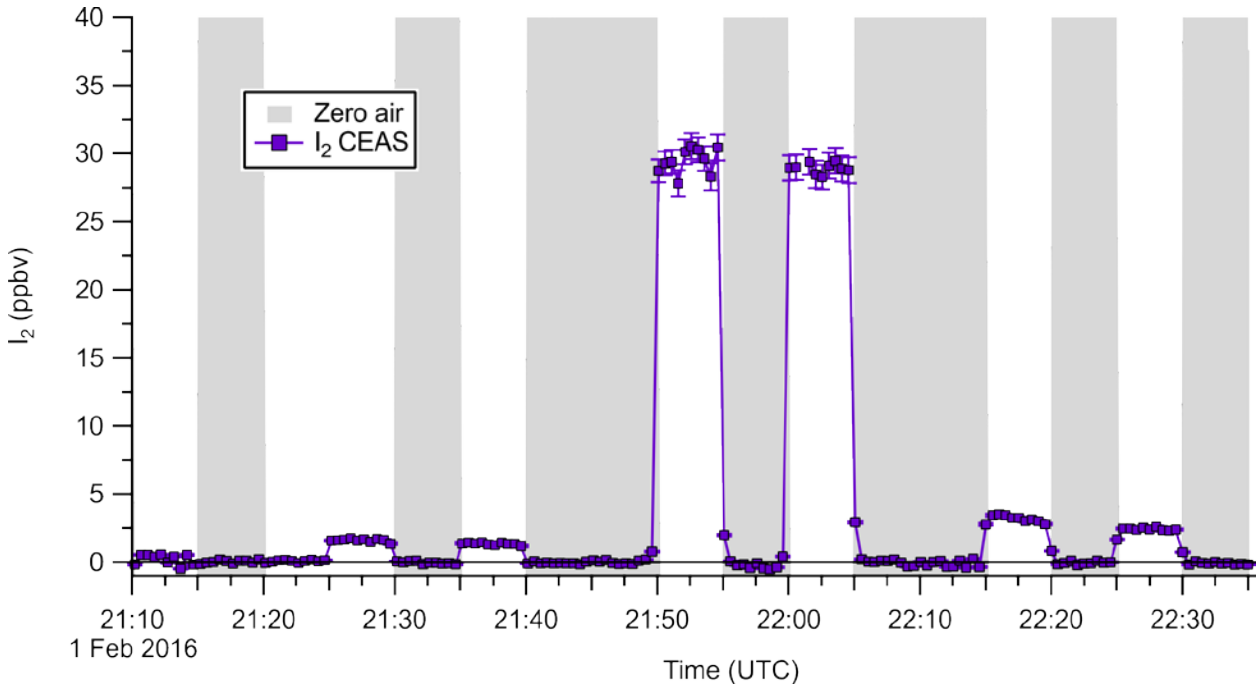

Figure S6 Time series of CEAS retrievals while sampling laboratory generated I_2. The grey underlay indicates times when the instrument sampled zero air. Iodine was delivered from four permeation tubes of different wall thickness, which were exchanged during the zeroing periods while the diffusion chamber output was bypassed.

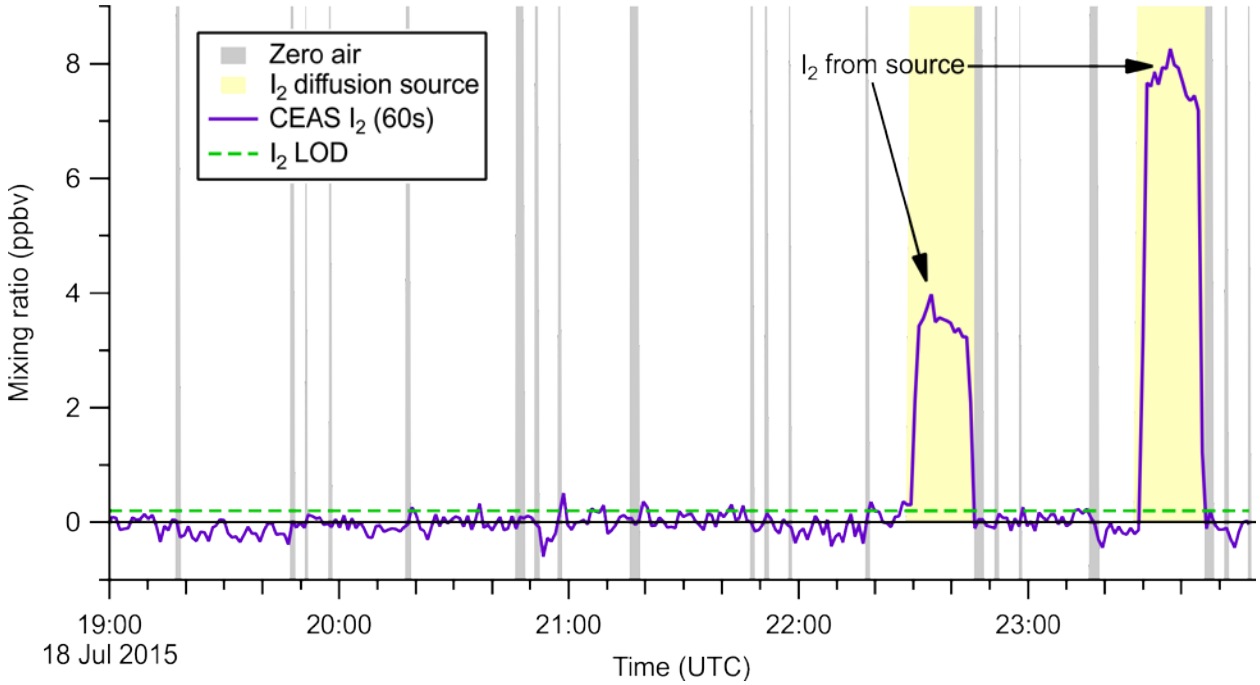

Figure S7 Time series of ambient air I_2 measurements during the ORCA campaign. The green dashed line represents the 2σ LOD for I_2. The grey shaded areas indicate periods when the CEAS sampled zero air. The yellow shaded areas indicate times when the CEAS sampled I_2 from a permeation which was controlled to a temperature of 40 °C at 22:30 and 55 °C at 23:30 UTC.

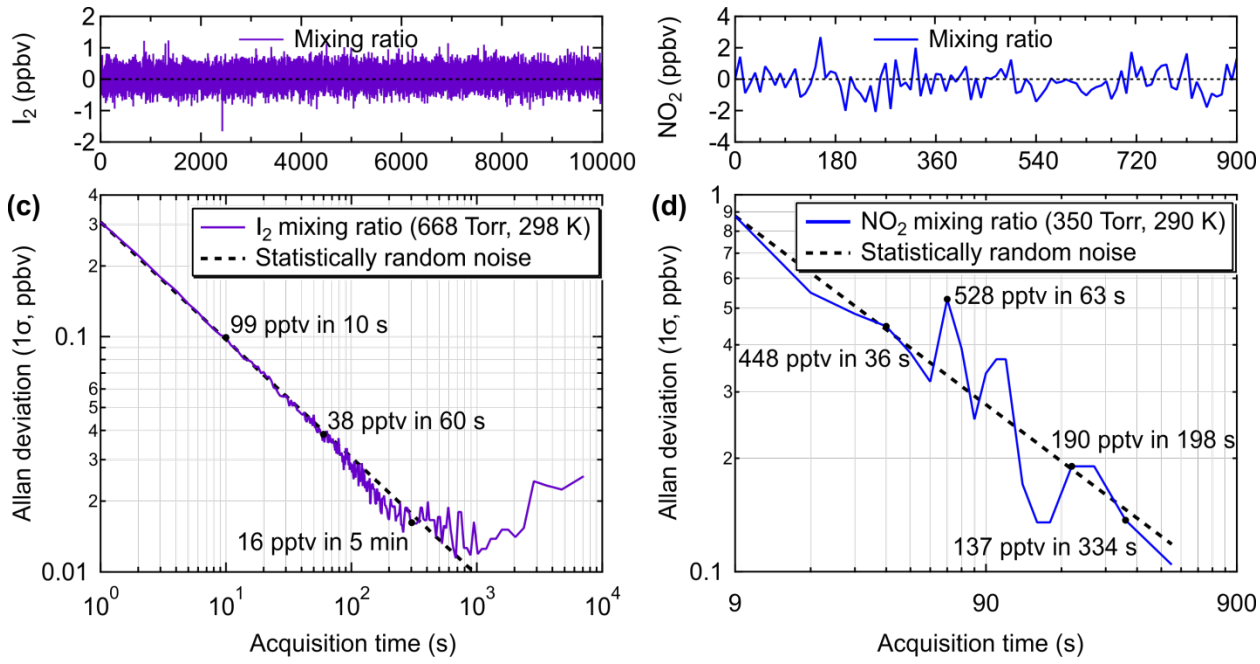

Figure S8 Allan deviation plots of Allan deviation plots of data collected while the CEAS was sampling zero air to determine the optimum integration time of: (**a)** a single pixel at 500 nm in the lab at 668 Torr (1.5 slpm sample rate) and 298 K, and **(b)** NO_2 mixing ratios during the ORCA campaign at 350 Torr (5 slpm sample rate) and 290 K.

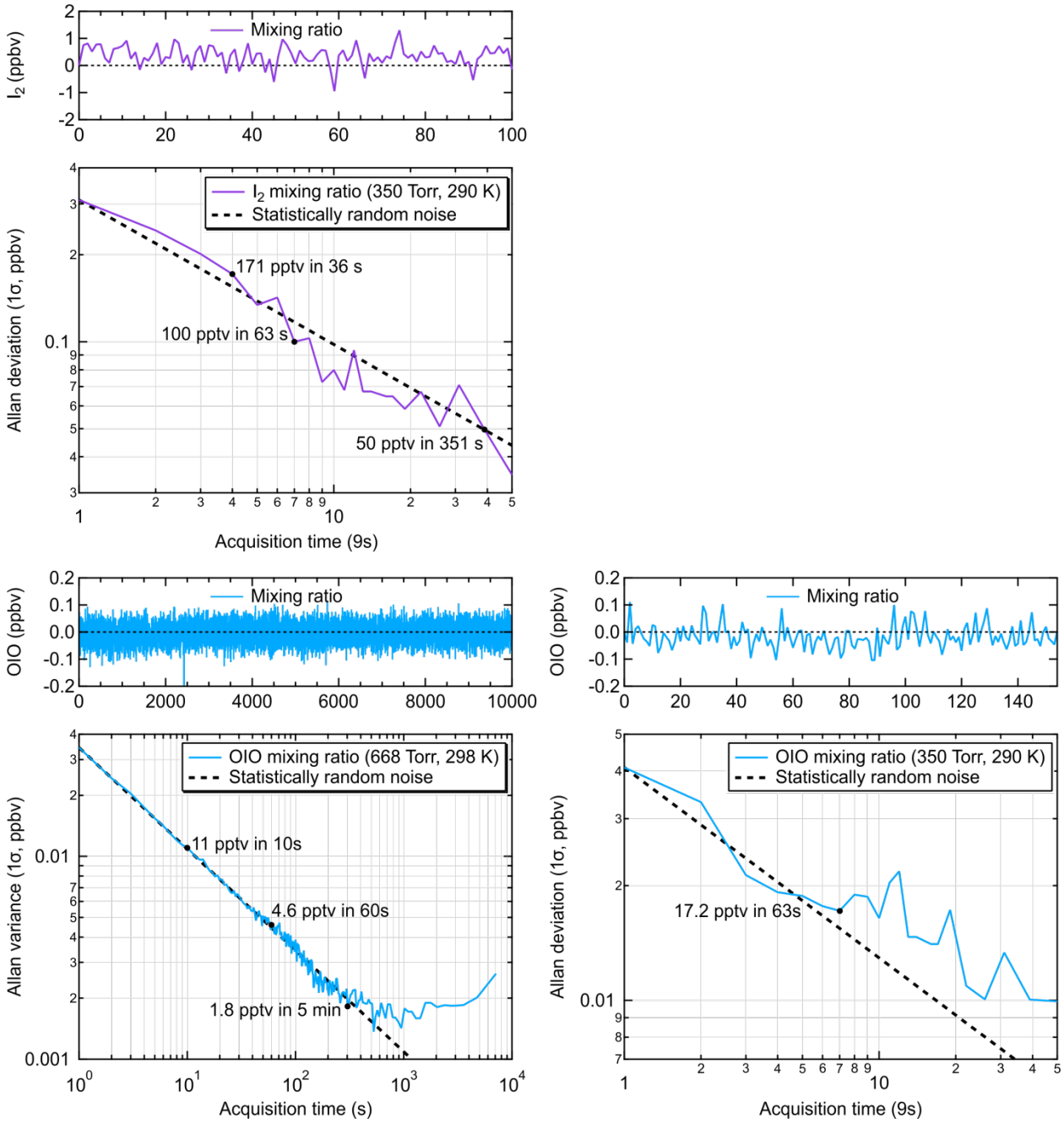

Figure S9 Allan deviation plots of data collected while the CEAS was sampling zero air to determine the optimum integration time and detection limits of: (**top**) I_2 during ambient sampling conditions; (**bottom left)** the calculated OIO mixing ratios in the lab at 668 Torr (1.5 slpm sample rate) and 298 K, and **(bottom right)** OIO mixing ratios during the ORCA campaign at 350 Torr (5 slpm sample rate) and 290 K.

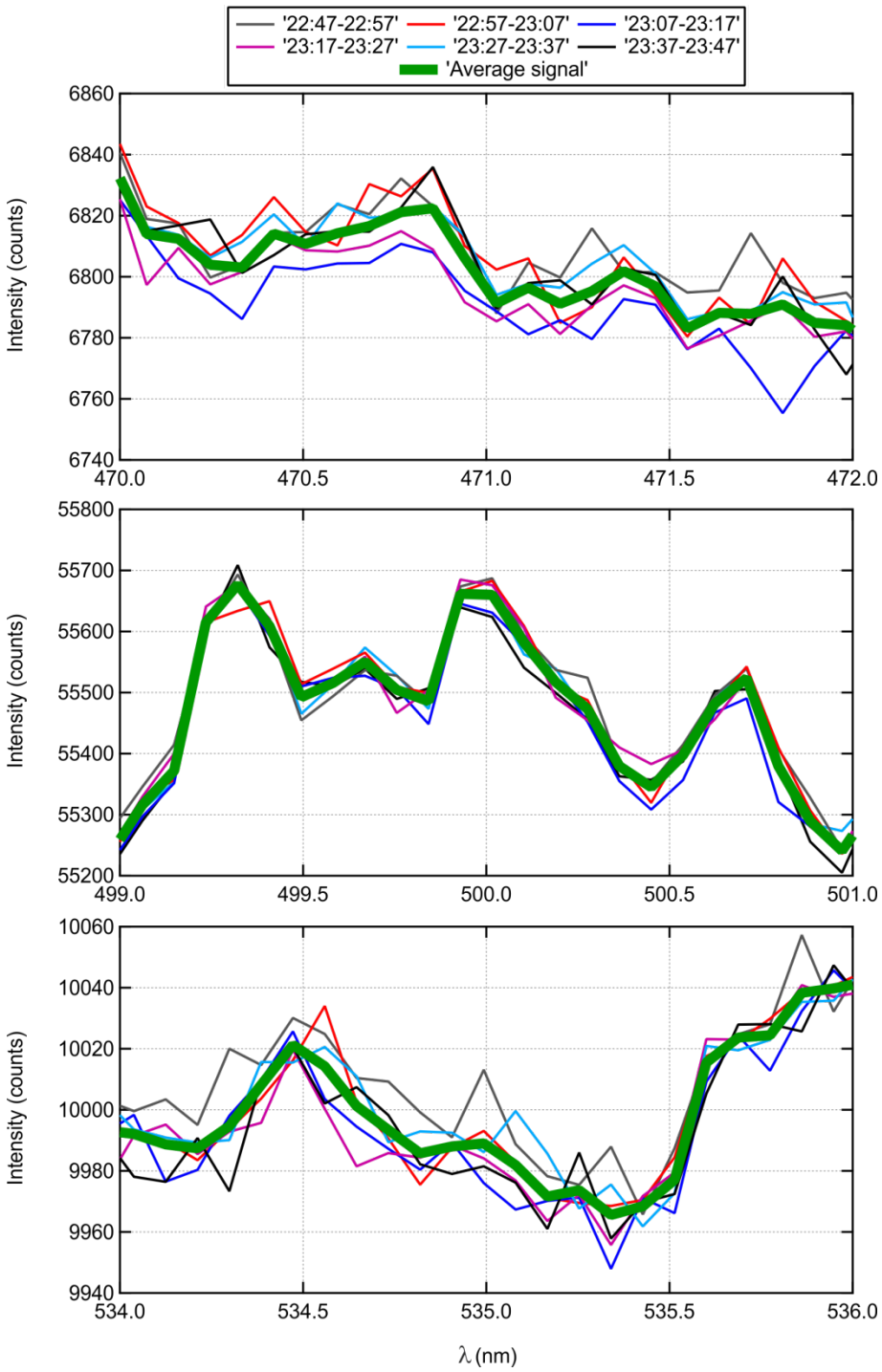

Figure S10 CEAS emission profile for a cavity filled with zero air and a LED (M505L3) driven at 30.0±0.1 °C. The stability of the emission profile was monitored over a 60 min interval with a LED warm up time of 30 min prior to measurements. Each trace represents a 10 min average while the thick green trace shows 60 min average.

References

Greenblatt, G. D., Orlando, J. J., Burkholder, J. B., and Ravishankara, A. R.: Absorption Measurements of Oxygen Between 330 and 1140 nm, J. Geophys. Res., 95, 18577–18582, 10.1029/JD095iD11p18577, 1990.

Hermans, C., Vandaele, A. C., Carleer, M., Fally, S., Colin, R., Jenouvrier, A., Coquart, B., and Mérienne, M.-F.: Absorption cross-sections of atmospheric constituents: NO_2, O_2, and H_2O, Environm. Sci. Poll. Res., 6, 151-158, 10.1007/bf02987620, 1999.

Newnham, D. A., and Ballard, J.: Visible absorption cross sections and integrated absorption intensities of molecular oxygen (O_2 and O_4), J. Geophys. Res.-Atmos., 103, 28801-28815, 10.1029/98JD02799, 1998.

Savitzky, A., and Golay, M. J. E.: Smoothing and Differentiation of Data by Simplified Least Squares Procedures, Anal. Chem., 36, 1627-1639, 10.1021/ac60214a047, 1964.

Sneep, M., and Ubachs, W.: Direct measurement of the Rayleigh scattering cross section in various gases, J. Quant. Spectrosc. Radiat. Transfer, 92, 293-310, 10.1016/j.jqsrt.2004.07.025, 2005.

Sneep, M., Ityaksov, D., Aben, I., Linnartz, H., and Ubachs, W.: Temperature-dependent cross sections of O_2-O_2 collision-induced absorption resonances at 477 and 577 nm, J. Quant. Spectrosc. Radiat. Transf., 98, 405-424, 10.1016/j.jqsrt.2005.06.004, 2006.

Thalman, R., and Volkamer, R.: Temperature dependent absorption cross-sections of O_2-O_2 collision pairs between 340 and 630 nm and at atmospherically relevant pressure, Physical Chemistry Chemical Physics, 15, 15371-15381, 10.1039/c3cp50968k, 2013.